Phase Transformation of the Periodic Mesoporous Organosilicas Assisted by Organotrialkoxysilane

Guiru Zhu, Qihua Yang,* Hua Zhong, Dongmei Jiang, and Can Li*

State Key Laboratory of Catalysis, Dalian Institute of Chemical Physics, Chinese Academy of Sciences, 457 Zhongshan Road, Dalian 116023, China

Received: March 9, 2007; In Final Form: May 16, 2007

A phase transformation of mesoporous organosilicas from 2D-hexagonal *P*6*mm* to cubic *Pm*3*n* phase can be induced by the organotrialkoxysilane with hydrophilic pendant group with the aid of methanol during the co-condensation of 1,2-bis(trimethoxysilyl)ethane (BTME) and $(EtO)_3Si$-R (R = L-prolinamide, *trans*-(1*R*,2*R*)-diaminocyclohexane, and γ-aminopropyl) using the cationic surfactant, octadecyltrimethylammonium chloride (C_{18}TMACl), as template in basic medium. Under similar synthesis conditions, no cubic *Pm*3*n* phase could be formed in the absence of $(EtO)_3Si$-R. Depending on the type of the pendant group, different amounts of methanol were needed for the formation of the cubic *Pm*3*n* phase. *N*-[(triethoxysilyl)propyl]-L-prolinamide (M_{L-Pro}) could easily induce the phase changing from 2D-hexagonal *P*6*mm* to cubic *Pm*3*n* phase probably because L-proline could result in a decreasing of the surfactant packing factor (*g*) through formation of large architecture on the outer boundary of the surfactant micelles. The organotrialkoxysilane can also help the formation of spherical morphology of the resultant materials.

Introduction

The periodic mesoporous organosilicas (PMOs) synthesized from $(R'O)_3Si$-R-$Si(OR')_3$[1−3] exhibit unique properties, such as enhanced hydrothermal, chemical, and mechanical stability.[4−6] Recently, the application of mesoporous organosilica spheres as packing materials in high-performance liquid chromatography (HPLC) has been demonstrated by our and other research groups.[7−9] Also, the PMOs with chiral ligand incorporated either in the mesoporous framework or in the mesopore were prepared.[10−15] These chiral PMOs exhibit chiral inductivity in the heterogeneous asymmetric catalysis. Compared with the mesoporous silicas, the PMOs are more attractive in the fields of catalysis, adsorption, chromatography, and so on.

Lots of efforts have been devoted on the structural and morphological control of PMOs. However, most PMOs reported have MCM-41[1−3,16−19] or SBA-15[20−24] type mesostructure consisting of a uniform one-dimensional channel, which will hamper the mass transfer during their applications in catalysis and separation. The cubic *Pm*3*n* phase (SBA-1) is very unique because of its cage-type pore structure with open windows.[25,26] It is generally accepted that a cubic mesostructure is more advantageous in view of the mass transfer than a hexagonal mesostructure, since the three-dimensional pore arrangements of the former are more resistant to pore blocking and allow faster diffusion of the reactants. The PMOs with cubic *Pm*3*n* symmetry were first synthesized from 1,2-bis(trimethoxylsilyl)ethane (BTME) using C_{16}TMACl as template under highly alkaline conditions.[27] The author found that the alkyl-chain length of the surfactant and the synthesis temperature were crucial parameters for the phase formation of the final product. No cubic *Pm*3*n* phase could be formed using C_{18}TMACl as template.[1,28] The structural and morphological control of the PMOs remains a field in need of investigation compared with the mesoporous silicas.

The organotrialkoxysilane (*N*-trimethoxysilylpropyl-*N*,*N*,*N*-trimethylammonium chloride or 3-aminopropyltrimethoxysilane) was recently employed as a special kind of cosurfactant for the synthesis of mesoporous silicas with special structure (chiral channels) or morphology (budded, mesoporous hollow spheres).[29,30] A phase transformation from the hexagonal structure to the cubic *Ia*3*d* structure was observed in the presence of a higher molar percent of organotrialkoxysilane during the co-condensation of tetraethoxysilane (TEOS) and triethoxyvinylsilane/3-mercaptopropyltrimethoxysilane using the triblock copolymer Pluronic P123 ($EO_{20}PO_{70}EO_{20}$) as structure directing agent in an acid medium.[31−34] The pronounced influence of the organotrialkoxysilane on the phase transformation is attributed to the hydrophobic pendant organic group, which will be preferentially adsorbed close to the hydrophobic poly(propylene oxide) (PPO) portion of the micelles and, therefore, cause a decrease in the preferential interfacial curvature, eventually favoring the formation of the *Ia*3*d* phase. To understand and investigate the role of the organotrialkoxysilane with different types of pendant organic groups in the phase formation is interesting because we could control the composition and structure of the mesoporous materials simultaneously.

It is considered that the morphology and structure of the mesoporous materials could be controlled through modifying the rigidity and curvature of the interfaces by different surfactant/silicate ratios, varying the temperature and pH of the reaction medium, and adding counterions and cosolvent/cosurfactant.[35−40] In this paper, we report the phase transformation of the mesoporous organosilicas induced by organotrialkoxysilane. The role of the organotrialkoxysilane, *N*-[(triethoxysilyl)propyl]-*trans*-(1*R*,2*R*)-diaminocyclohexane (M_{DACH}), *N*-[(triethoxysilyl)-propyl]-L-prolinamide (M_{L-Pro}), and 3-aminopropyltriethoxysilane in the structural and morphological evolution was investigated. We found that the hydrophilic pendant group could

* To whom correspondence should be addressed. E-mail: yangqh@dicp.ac.cn (Q. H. Yang), canli@dicp.ac.cn (C. Li). Home page: http://www.hmm.dicp.ac.cn, http://www.canli.dicp.ac.cn. Fax: 86-411-84694447.

10.1021/jp071913j CCC: $37.00
Published on Web 06/26/2007

assist the formation of cubic *Pm*3*n* phase and spherical morphology with the aid of methanol.

Experimental Section

Chemicals. 1,2-Bis(trimethoxysilyl)ethane (BTME) and 3-aminopropyltriethoxysilane (APTES) were purchased from Sigma-Aldrich. Octadecyltrimethylammonium chloride (C_{18}TMACl) was from Nanjing Robiot (Nanjing, China). The other reagents were purchased from Shanghai Chemical Reagent of Chinese Medicine Group (Shanghai, China). *trans*-(1*R*,2*R*)-Diaminocyclohexane (DACH) was prepared by resolving the commercially available mixture of *cis*- and *trans*-diaminocyclohexane (30/70) according to the literature.[41] All solvents are of analytical quality and were dried by standard methods. *N*-[(Triethoxysilyl)-propyl]-*trans*-(1*R*,2*R*)-diaminocyclohexane (M_{DACH})[42] and *N*-[(triethoxysilyl)propyl]- L-prolinamide (M_{L-pro})[43] were synthesized according to the published method.

Synthesis. In a typical synthesis of L-proline-functionalized mesoporous ethane−silicas (L-Pro-MES), C_{18}TMACl (1.04 g) was dissolved in a mixture of water (20.0 mL) and desired amounts of MeOH and NaOH (1 M, 11.8 mL) at 40 °C. After being cooled down to room temperature, the mixture of M_{L-pro} (0.32 g) and BTME (1.08 g) was added to the above solution under vigorous stirring. After being stirred for 30 min at room temperature, the clear solution was transferred into a Teflon-lined autoclave and kept at 80 °C for 16 h without agitation. The white precipitate was collected by filtration, washed thoroughly with deionized water, and dried at 60 °C. The molar ratio of the compositions for the synthesis is $0.20M_{L-pro}$/0.80BTME/$0.60C_{18}$TMACl/2.36NaOH/$353.6H_2O$/*x* methanol. The sample was denoted as L-Pro-MES-*x*, where *x* refers to the molar ratio of methanol/(BTME + R-Si$(OEt)_3$). The surfactant was extracted by stirring 1.0 g of as-synthesized sample in 200 mL of ethanol containing 2.05 g of 36% HCl for 6 h at 50 °C. After filtration, the sample was washed thoroughly with ethanol and dried in air at 60 °C overnight.

M_{DACH} and APTES were also used as organotrialkoxysilane for the synthesis of DACH- and NH_2-functionalized mesoporous ethane−silicas, respectively. The synthetic conditions and compositions were similar to that of L-Pro-MES-*x*. The DACH- and NH_2-functionalized mesoporous ethane−silicas were denoted as DACH-MES-*x* and NH_2-MES-*x*, respectively, where *x* refers to the molar ratio of methanol/(BTME + R-Si$(OEt)_3$).

For comparison, the mesoporous ethane−silicas (MES-*x*) were synthesized from BTME without the addition of organotrialkoxysilane. The synthetic conditions and compositions are similar to those of L-Pro-MES, where *x* refers to the molar ratio of methanol/(BTME).

Characterization. Scanning electron microscopy (SEM) images were realized on a JSM-6360 microscope operated at an accelerating voltage of 20−30 kV. The samples were deposited on a sample holder with an adhesive carbon foil and sputtered with gold prior to imaging. A transmission electron microscopy (TEM) image was obtained on a Philips Tecnai G^2 20 electron microscope operated at an acceleration voltage of 200 kV. Powder X-ray diffraction (XRD) patterns were recorded on a Rigaku D/Max 3400 powder diffraction system using Cu Kα radiation. Nitrogen sorption experiments were performed at 77 K on an ASAP 2000 analyzer. The samples were pretreated at 100 °C before the measurement. Brunauer−Emmett−Teller (BET) surface areas were calculated from adsorption data in the relative pressure (P/P_0) range of 0.01−0.2. The pore-size distribution curves were obtained from the adsorption branches using the Barrett−Joyner−Halenda (BJH) method.

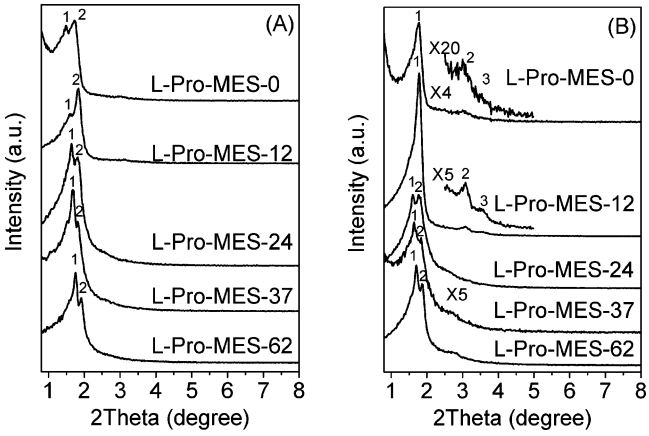

Figure 1. XRD patterns of the L-Pro-MES-*x* synthesized by co-condensation of BTME and *N*-[(triethoxysilyl)propyl]-L-prolinamide (M_{L-Pro}) in the presence of different concentrations of methanol before (A) and after (B) surfactant extraction.

Results and Discussion

Influence of Organotrialkoxysilane and Methanol on the Phase Formation of the Mesoporous Organosilicas. XRD patterns for L-Pro-MES-*x* synthesized with different amounts of methanol before and after surfactant extraction are shown in Figure 1. The d-spacings are listed in Table 1. The XRD pattern of as-synthesized L-Pro-MES-0 shows two peaks with similar intensity in the low-angle region, whereas the extracted L-Pro-MES-0 exhibits three diffraction peaks in the low-angle region, which could be assigned to (100), (110), and (210) diffractions of a typical 2D-hexagonal *P*6*mm* mesostructure. The XRD results indicate that the as-synthesized L-Pro-MES-0 consists of mixed mesophases. One of the mesophases is not stable; it transforms into *P*6*mm* phase during the surfactant-extraction process. The phase transformation of mesoporous silicas during the processes of drying and calcination is often observed, especially for SBA-1.[44−46] Under similar reaction conditions, the as-synthesized or extracted MES-0 synthesized from BTME (without the addition of M_{L-Pro}) exhibits three diffraction peaks at the low-angle region, which could be assigned to (100), (110), and (210) diffractions of a typical 2D-hexagonal *P*6*mm* mesostructure (Figure 2). This suggests that the presence of M_{L-Pro} can assist the phase changing.

Alcohol was a general cosolvent for the synthesis of cubic *Pm*3*n* phase under acidic conditions. Therefore, methanol was added with an aim to further accelerate the phase changing from 2D-hexagonal structure to cubic *Pm*3*n* phase. However, the as-synthesized or extracted MES-62 still has *P*6*mm* phase, as evidenced by the presence of three diffraction peaks in its XRD pattern (Figure 2). The XRD pattern of as-synthesized MES-100 exhibits two diffraction peaks. After surfactant extraction, only one sharp diffraction peak was observed. The above results indicate that it is very difficult to obtain cubic *Pm*3*n* phase for MES-*x*, even in the presence of large amounts of methanol.

Two diffraction peaks were observed in the XRD patterns of as-synthesized L-Pro-MES-12 and L-Pro-MES-24 (synthesized with the addition of small amounts of methanol), which is similar to that seen for L-Pro-MES-0 (Figure 1A). After surfactant extraction, L-Pro-MES-12 shows an XRD pattern with three well-resolved peaks in the region of $2\theta = 1.5-4°$, which are indexed to (100), (110), and (210) diffractions of a typical 2D-hexagonal *P*6*mm* mesostructure (Figure 1B). However, after surfactant extraction, the XRD pattern of L-Pro-MES-24 shows two main reflections corresponding to the (210) and (211)

TABLE 1: *d*-Spacings and Phase Assignment of the Mesoporous Organosilicas before and after Surfactant Extraction[a]

sample	d_1 (Å)	d_2 (Å)	d_3 (Å)	peak assignment[b]	mesophase
L-Pro-MES-0	59.63 (50.16)	51.31 (29.23)	(24.88)	un[c] (100/110/210)	mixed (*P*6*mm*)
L-Pro-MES-12	55.16 (49.59)	48.01 (28.67)	(25.08)	un (100/110/210)	mixed (*P*6*mm*)
L-Pro-MES-24	53.80 (55.13)	48.50 (50.14)		un (210/211)	mixed (*Pm*3*n*)
L-Pro-MES-37	53.15 (52.56)	49.04 (47.99)		210/211 (210/211)	*Pm*3*n* (*Pm*3*n*)
L-Pro-MES-62	50.20 (51.59)	46.00 (47.45)		210/211 (210/211)	*Pm*3*n* (*Pm*3*n*)
DACH-MES-24	47.99 (48.49)	28.10 (28.29)	24.06 (24.35)	100/110/210 (100/110/ 210)	*P*6*mm* (*P*6*mm*)
DACH-MES-49	54.49 (54.47)	47.39 (46.94)		un (un)	mixed (mixed)
DACH-MES-62	50.17 (51.33)	46.01 (46.98)		210/211 (210/211)	*Pm*3*n* (*Pm*3*n*)
NH_2-MES-24	48.52 (50.15)	28.12 (28.85)	24.53 (24.95)	100/110/210 (100/110/ 210)	*P*6*mm* (*P*6*mm*)
NH_2-MES-37	52.50 (55.17)	46.00 (48.54)		un (un)	mixed (mixed)
NH_2-MES-62	49.64 (51.92)	45.99 (47.48)		210/211 (210/211)	*Pm*3*n* (*Pm*3*n*)

[a] Data in the parentheses refer to the surfactant extracted sample. [b] The diffraction peaks with the d-spacings having the relationship of $1:\sqrt{3}:2$ can be indexed to the 100, 110, and 200 diffraction peaks of a *P*6*mm* mesostructure. The diffraction peaks with the d-spacings having the relationship of $\sqrt{5}:\sqrt{6}$ can be indexed to the 210 and 211 diffraction peaks of a *Pm*3*n* mesostructure. [c] The mesophase cannot be assigned to any known phase according to the relationship of d-spacings of the diffraction peak.

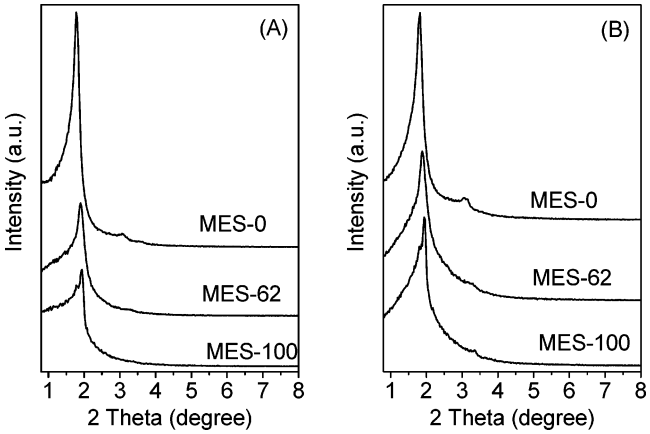

Figure 2. XRD patterns of ethane-silica (MES-*x*) synthesized by condensation of BTME in the presence of different concentration of methanol before (A) and after (B) surfactant extraction.

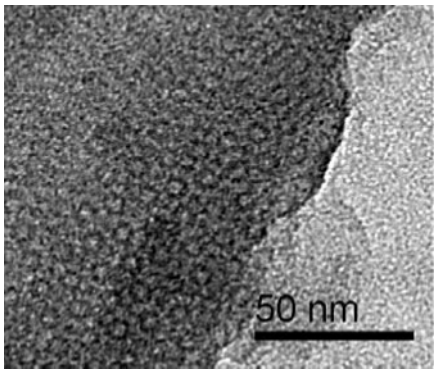

Figure 3. TEM image of L-Pro-MES-62.

diffraction of cubic *Pm*3*n* phase (Figure 1B). It indicates that *x* of 24 is the transition point for the phase changing from 2D-hexagonal *P*6*mm* to cubic *Pm*3*n*. L-Pro-MES-37 and L-Pro-MES-62 have a cubic *Pm*3*n* phase before and after surfactant extraction. Compared with L-Pro-MES-24 and L-Pro-MES-37, the mesostructure of L-Pro-MES-62 is more ordered, suggesting that higher amounts of methanol favor the formation of a highly ordered cubic *Pm*3*n* phase. The mesostructure of L-Pro-MES-62 was further characterized by TEM technique (Figure 3). The TEM image of L-Pro-MES-62 was taken along the (100) direction. It clearly reveals the well-defined edges with a spherical shape, suggesting that the sample has the cubic *Pm*3*n* symmetry.[27,46] Compared with MES-*x*, we could see that the phase changing from *P*6*mm* to *Pm*3*n* is pronounced by the addition of M_{L-Pro}.

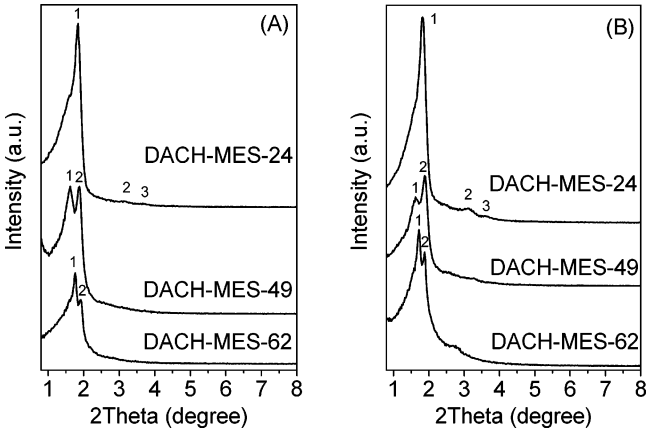

Figure 4. XRD patterns of the DACH-MES-*x* synthesized by co-condensation of BTME and *N*-[(triethoxysilyl)propyl]-*trans*-(1*R*,2*R*)-diaminocyclohexane (M_{DACH}) in the presence of different concentrations of methanol before (A) and after (B) surfactant extraction.

The previous studies show that thiol and vinyl group can help the formation of the cubic *Ia*3*d* structure because of their hydrophobicity, when the triblock copolymer Pluronic P123 was used as the surfactant in acidic medium.[31−34] The L-proline is more hydrophilic compared with thiol and vinyl group. To understand the mechanism of the phase changing induced by M_{L-Pro}, the influence of other organotrialkoxysilanes, such as M_{DACH} and APTES (with the hydrophilic pendant group), on the phase formation of the mesoporous organosilicas was investigated.

Figure 4 displays the XRD patterns of DACH-MES-*x*. The d-spacings are listed in Table 1. The XRD patterns of DACH-MES-24 before and after surfactant extraction exhibit three diffraction peaks in the low-angle region, characteristic of mesoporous materials with typical 2D-hexagonal *P*6*mm* phase. Two diffraction peaks with similar intensity were observed in the XRD pattern of as-synthesized DACH-MES-49. After surfactant extraction, the two diffraction peaks still remain with a slight change of the intensity ratio. From the calculation, we could see that DACH-MES-49 has mixed phases. The XRD patterns of DACH-MES-62 before and after extraction clearly show the existence of (210) and (211) diffractions, suggesting that DACH-MES-62 has the cubic *Pm*3*n* phase. The XRD results show that M_{DACH} could also induce a phase changing from 2D-hexagnol *P*6*mm* to cubic *Pm*3*n*. APTES with hydrophilic $-CH_2CH_2CH_2NH_2$ was also used for the synthesis of the mesoporous materials. NH_2-MES-24 before and after extraction has *P*6*mm* phase, as evidenced from the three diffraction peaks in their XRD patterns (Figure 5). A mixed phase was observed

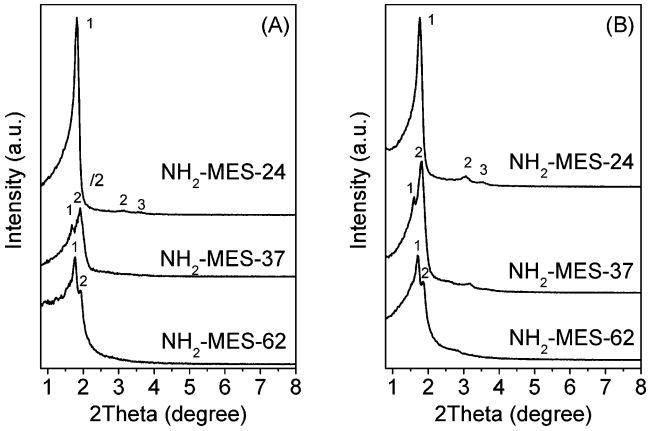

Figure 5. XRD patterns of the NH_2-MES-*x* synthesized by co-condensation of BTME and 3-aminopropyltrimethoxysilane (APTES) in the presence of different concentrations of methanol before (A) and after (B) surfactant extraction.

TABLE 2: Synthetic Details and Physical Parameters of the Mesoporous Organosilicas

sample[a]	methanol/(BTME+R-Si(OEt)$_3$) (mol/mol)	BET surface area (m^2/g)	pore volume (cm^3/g)	pore size[b] (nm)
L-Pro-MES-0	0	975	0.88	2.80
L-Pro-MES-12	12	1146	1.01	2.77
L-Pro-MES-24	24	873	0.63	2.82
L-Pro-MES-37	37	920	0.67	2.77
L-Pro-MES-62	62	1142	0.80	2.58
DACH-MES-24	24	880	0.74	3.01
DACH-MES-49	49	885	0.67	3.13
DACH-MES-62	62	978	0.70	2.99
NH_2-MES-24	24	817	0.76	2.80
NH_2-MES-37	37	1011	0.93	2.80
NH_2-MES-62	62	834	0.70	2.61

[a] All samples prepared with 0.20R-Si(OEt)$_3$/0.80BTME/0.60C_{18}TMCl/2.36NaOH/353.6H_2O/*x*MeOH. [b] Calculated from the adsorption branch using the BJH method.

when *x* reaches 37. The XRD pattern of NH_2-MES-62 implies that this sample has cubic *Pm*3*n* phase. Therefore, a phase changing from *P*6*mm* to cubic *Pm*3*n* could be induced by APTES. The pendant group of M_{L-Pro} and M_{DACH} has the carbon ring, while APTES has the pendant group with the carbon chain. All these organotriethoxysilane precursors could induce a phase changing. For the formation of cubic *Pm*3*n* phase, higher amounts of methanol were needed in the presence of M_{DACH} and APTES than in the presence of M_{L-Pro}, suggesting that M_{L-Pro} is the most suitable precursor for accelerating the phase changing.

All materials exhibit type IV isotherm patterns, characteristic of the mesoporous materials with uniform pore-size distributions. The physical parameters of L-Pro-MES-*x*, DACH-MES-*x*, and NH_2-MES-*x* were summarized in Table 2. All the mesoporous materials have high BET surface area and large pore volume. The pore diameter changes irregularly with the amounts of methanol. The DACH-MES-*x* has the largest pore diameter among all the materials synthesized under similar synthetic conditions.

From the results of XRD and TEM, we could see that a phase changing from 2D-hexaganol *P*6*mm* to cubic *Pm*3*n* mesophase could be induced by the presence of M_{L-Pro}, M_{DACH}, and APTES. M_{L-Pro}, M_{DACH}, and APTES have the hydrophilic pendant group, but with different functional groups. Without the addition of organotrialkoxysilane, no cubic *Pm*3*n* could be formed from BTME under the current synthetic conditions. Also,

SCHEME 1: Illustrated Phase Formation of the Mesoporous Organosilicas

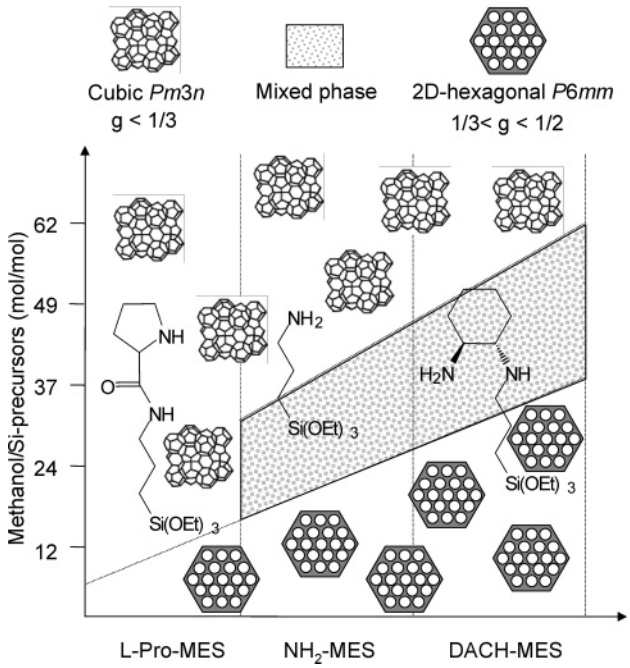

we found that the amounts of methanol needed for the synthesis of mesoporous organosilicas with cubic *Pm*3*n* decrease in the following order: L-Pro-MES < NH_2-MES < DACH-MES. The influence of organotrialkoxysilane and methanol on the phase changing has been depicted in Scheme 1.

Proposed Mechanism for the Phase Formation of the Mesoporous Organosilicas. The phase transformation can be explained by the changes of surfactant packing parameter, *g*, which was dedicated by Huo et al.[26] This surfactant packing parameter *g* directs the phase configuration in the synthesis of mesoporous material. The *g* is defined as $g = V/(a_0 l)$, where *V* is the total volume of surfactant chains plus any cosolvent organic molecules between the chains, a_0 is the effective headgroup area at the organic−inorganic interface, and *l* is the surfactant chain length. Small values of *g* favor a phase with more curved surfaces such as cubic *Pm*3*n* ($g < 1/3$) and hexagonal *P*6*mm* ($1/3 < g < 1/2$), while large values of *g* favor structures with smaller curvature such as cubic *Ia*3*d* ($1/2 < g < 2/3$) and lamellar *P*2 ($g = 1$).

Previous studies of Inagaki and co-workers[27] show that the mesoporous ethane−silica with cubic *Pm*3*n* structure could be formed using C_{16}TMA as surfactant under basic conditions. When C_{18}TMA was used as surfactant, only *P*6*mm* phase was observed.[1,28] The ethane moiety bridged between two silicons in BTME is hydrophobic; therefore, it can penetrate into the hydrophobic core of the surfactant micelles. The *V* will be increased, which may inhibit the formation of cubic *Pm*3*n* phase. This may be the reason that the cationic surfactant with short carbon was needed for the synthesis of cubic *Pm*3*n* ethane−silica. The hydrophilic methanol residing on the outer boundaries of the surfactant micelles results in an enlargement of the effective headgroup area (a_0) and, thus, decreases the *g* value and favors the formation of cubic *Pm*3*n* phase. However, we still cannot get cubic *Pm*3*n* ethane−silica, even with the addition of large amounts of methanol, when C_{18}TMA is used as surfactant. This indicates that the increased *V* by BTME cannot be compensated by the addition of methanol. The hydrophilic molecule of large size may be needed to reduce *g* value through increasing a_0.

Similar to methanol, M_{L-Pro} with the hydrophilic pendant group can only reside on the outer boundaries of the surfactant micelles. As a result, a diluting effect occurs and makes the surfactant micelles less packed, which effectively decreases the electrostatic repulsion among $C_{18}TMA^+$ ions in micelles. Under such conditions, a surfactant micelle with a high surface curvature is favored. Moreover, the pendant L-proline moiety may form strong hydrogen bonds between themselves and with methanol. The hydrogen bond of C═O···C_δH, C═O···OH, and NH···OH may lead to the formation of large architecture from M_{L-Pro} and methanol. Consequently, the size of the effective head group area (a_0) is much bigger in the presence of M_{L-Pro} than in the absence of M_{L-Pro}, which can result in the formation of cubic *Pm*3*n* phase.

The *trans*-(1*R*,2*R*)-diaminocyclohexane in M_{DACH} is hydrophilic and can also form a hydrogen bond. However, the configuration of *trans*-(1*R*,2*R*)-diaminocyclohexane is more rigid than that of L-proline. The pendant group ($-CH_2CH_2CH_2NH_2$) of APTES is also hydrophilic and can form a hydrogen bond. However, the molecular size is smaller than that of L-proline in M_{L-Pro}. Therefore, the formation of large architecture from M_{DACH} and APTES is not easy compared with that from M_{L-Pro}. This may be the reason that higher amounts of methanol were needed for the formation of the cubic *Pm*3*n* phase for DACH-MES-*x* and NH_2-MES-*x* than for L-Pro-MES-*x*.

From the above analysis, we can see that the presence of M_{L-Pro}, M_{DACH}, and APTES with a hydrophilic pendant group can induce the formation of cubic *Pm*3*n* phase through decreasing the *g* value. The cubic *Pm*3*n* phase is more easily induced by the pendant group with the ability for the formation of large architecture. Through adjusting the methanol amounts, the cubic (*Pm*3*n* phase) mesoporous ethane−silicas with functional groups in the mesopore can be successfully synthesized.

Morphology Evolution Induced by Organotrialkoxysilane and Methanol. The morphology of MES-*x* and L-Pro-*x* was investigated using the SEM technique (Figure 6). The methanol has a big influence on the morphology of L-Pro-MES-*x*. With the amounts of methanol increasing, the morphology of L-Pro-MES-*x* evolves gradually from polyhedron (L-Pro-MES-0), to cakelike particles (L-Pro-MES-12 and L-Pro-MES-24), and to spherelike particles (L-Pro-MES-37). When *x* reaches 62, the monodispersed spheres with smooth surfaces were observed for L-Pro-MES-62. From the above results, we could see that the addition of methanol can result in the formation of monodispersed mesoporous spheres. The spherical L-Pro-MES-62 with L-proline ligand in the mesopore may be good candidates as chiral stationary phases for high-performance liquid chromatography. Under similar synthetic conditions to those of L-Pro-MES-62, MES-62 synthesized without the addition of M_{L-Pro} consisted of irregularly shaped particles, suggesting that the presence of M_{L-Pro} helps the formation of the spherical morphology.

The morphology of DACH-MES-*x* and NH_2-MES-*x* is displayed in Figure 7 and Figure 8, respectively. DACH-MES-24 consisted of ball-flower shaped particles. Cakelike and irregularly shaped particles coexist in DACH-MES-49. DACH-MES-62 has monodispersed spheres (Figure 7). The cakelike particles, the spheres with gyroids, and the monodispersed spheres were observed in the SEM images of NH_2-MES-24, NH_2-MES-37, and NH_2-MES-62, respectively (Figure 8). The SEM results indicate that the influence of methanol on the morphology evolution of L-Pro-MES-*x*, DACH-MES-*x*, and NH_2-MES-*x* is almost the same.

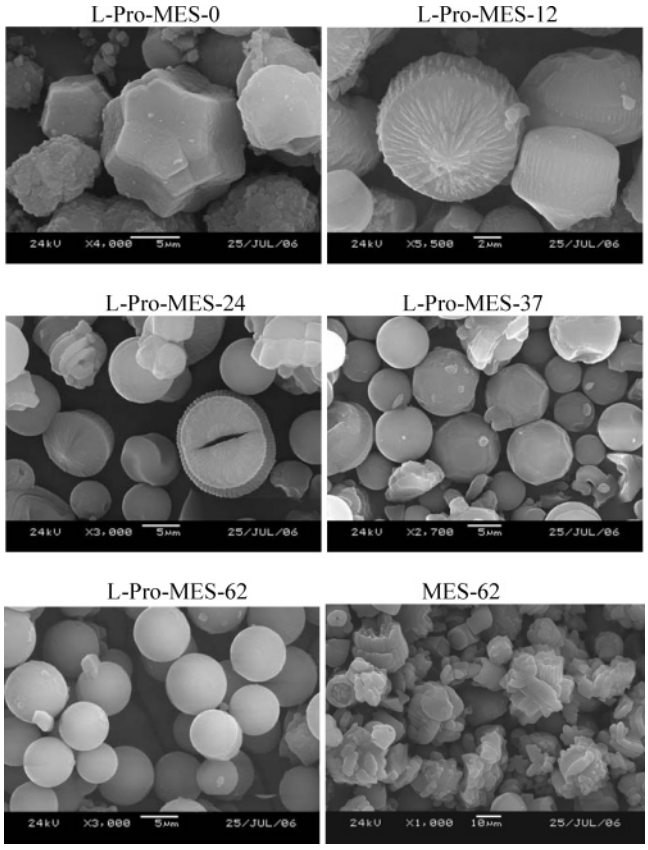

Figure 6. SEM images of surfactant-free mesoporous organosilicas synthesized in the presence of different concentrations of methanol.

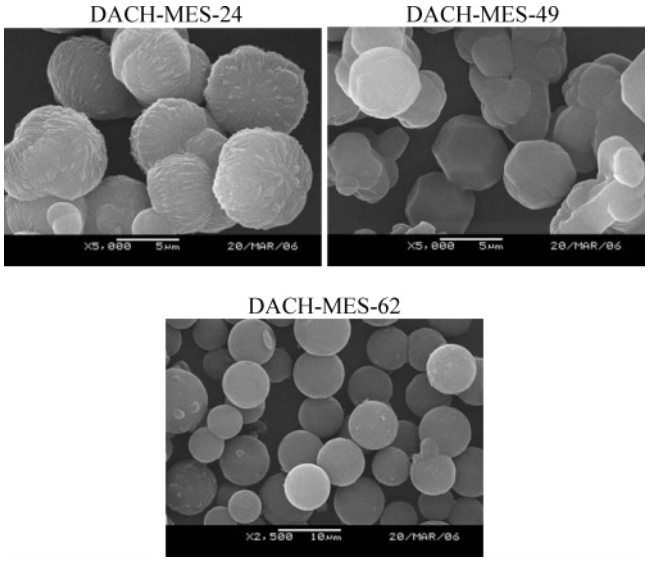

Figure 7. SEM images of surfactant-free DACH-MES-*x* synthesized in the presence of different concentrations of methanol.

With hydrophilic pendant groups, the organotrialkoxysilane (M_{L-Pro}, M_{DACH}, and APTES) can interact with each other through the hydrogen bond. The condensation of hydrolyzed $-Si(OH)_n(OR)_{3-n}$ species around the $C_{18}TMACl$ micelles may be slowed down because of the steric hindrance of the existence of hydrogen bonds between the organotrialkoxysilanes. The slow condensation rate of silane species is helpful for the formation of spheres;[47] therefore, the spheres with smooth surfaces can be formed in the presence of organotrialkoxysilane.

Higher amounts of methanol benefit the formation of spheres with smooth surfaces in the presence of organotrialkoxysilane.

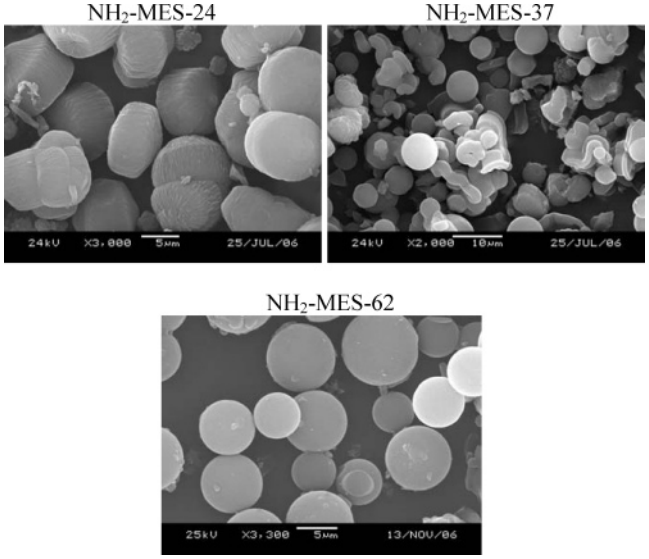

Figure 8. SEM images of surfactant-free NH_2-MES-*x* synthesized in the presence of different concentrations of methanol.

The addition of methanol may decrease the polarity of the solvent and retard the hydrolysis rates of the organosilane precursors because of a preferential solvating of the silane precursors into the alcohol phase. The slow condensation of the hydrolyzed silane species around the surfactant micelles induced by the addition of methanol also contributes to the formation of organosilica spheres with smooth surface.[48] The slow condensation rates of the hydrolyzed silane species around the surfactant micelles can be achieved in the presence of $(EtO)_3Si$-R with a hydrophilic pendant group at a higher concentration of methanol, which mainly contributes to the formation of spherical morphology.

Conclusions

In summary, a phase transformation from highly ordered 2D-hexagonal *P6mm* to cubic *Pm*3*n* phase was observed during the synthesis of mesoporous organosilicas with organic groups in the mesopore. The organotrialkoxylsilane precursor (M_{L-Pro}, M_{DACH}, and APTES) with the hydrophilic pendant group could result in the formation of cubic *Pm*3*n* phase with the help of methanol through decreasing the *g* value. M_{L-Pro} can greatly accelerate the formation of cubic *Pm*3*n* phase compared with that by M_{DACH} and APTES, as evidenced by the fact that a lower amounts of methanol were needed in the presence of M_{L-Pro}. The surfactant packing factor, *g*, could be effectively reduced by M_{L-Pro} through the formation of large architecture on the outer boundary of the surfactant micelles. The other organotrialkoxysilane precursors with a hydrophilic pendant organic group and the ability for the formation of a hydrogen bond may also induce the formation of the cubic *Pm*3*n* phase. The mesoporous organosilica spheres can also be obtained because of the slow hydrolysis and condensation rates of the silane precursors in the presence of organotrialkoxylsilane precursor (M_{L-Pro}, M_{DACH}, and APTES) with the hydrophilic pendant group and methanol.

Acknowledgment. This work is financially supported by the National Natural Science Foundation of China (20303020, 20321303, 20503028), National Basic Research Program of China (2003 CB 615803), and Knowledge Innovation Program of the Chinese Academy of Sciences (DICP K2003B2, K2006B2).

References and Notes

(1) Inagaki, S.; Guan, S.; Fukushima, Y.; Ohsuna, T.; Terasaki, O. *J. Am. Chem. Soc.* **1999**, *121*, 9611.
(2) Melde, B. J.; Holland, B. T.; Blanford, C. F.; Stein, A. *Chem. Mater.* **1999**, *11*, 3302.
(3) Asefa, T.; Maclachlan, M. J.; Coombs, N.; Ozin, G. A. *Nature* **1999**, *402*, 867.
(4) Lu, Y.; Fan, H.; Doke, N.; Loy, D. A.; Assink, R. A.; LaVan, D. A.; Brinker, C. J. *J. Am. Chem. Soc.* **2000**, *122*, 5258.
(5) Burleigh, M. C.; Markowitz, M. A.; Jayasundera, S.; Spector, M. S.; Thomas, C. W.; Gaber, B. P. *J. Phys. Chem. B* **2003**, *107*, 12628.
(6) Liu, J.; Yang, J.; Yang, Q. H.; Wang, G.; Li, Y. *Adv. Funct. Mater.* **2005**, *15*, 1297.
(7) Zhu, G. R.; Yang, Q. H.; Jiang, D. M.; Yang, J.; Zhang, L.; Li, C. *J. Chromatogr., A* **2006**, *1103*, 257.
(8) Kim, D.; Chung, J.; Ahn, W.; Kang, G.; Cheong, W. *Chem. Lett.* **2004**, *33*, 422.
(9) Rebbin, V.; Schmidt, R.; Fröba, M. *Angew. Chem., Int. Ed.* **2006**, *43*, 5210.
(10) Jiang, D. M.; Yang, Q. H.; Yang, J.; Zhang, L.; Zhu, G. R.; Su, W.; Li, C. *Chem. Mater.* **2005**, *17*, 6154.
(11) Jiang, D. M.; Gao, J.; Yang, Q. H.; Yang, J.; Li, C. *Chem. Mater.* **2006**, *18*, 6012.
(12) Álvaro, M.; Benitez, M.; Das, D.; Ferrer, B.; García, H. *Chem. Mater.* **2004**, *16*, 2222.
(13) Benitez, M.; Bringmann, G.; Dreyer, M.; García, H.; Ihmels, H.; Waidelich, M.; Wissel, K. *J. Org. Chem.* **2005**, *70*, 2315.
(14) Baleizão, C.; Gigante, B.; Das, D.; Álvaro, M.; García, H.; Corma, A. *Chem. Commun.* **2003**, 1860.
(15) Baleizão, C.; Gigante, B.; Das, D.; Álvaro, M.; García, H.; Corma, A. *J. Catal.* **2004**, *223*, 106.
(16) Nakajima, K.; Lu, D.; Kondo, J. N.; Tomita, I.; Inagaki, S.; Hara, M.; Hayashi, S.; Domen, K. *Chem. Lett.* **2003**, *32*, 950.
(17) Yoshina-Ishii, C.; Asefa, T.; Coombs, N.; MacLachlan, M. J.; Ozin, G. A. *Chem. Commun.* **1999**, 2539.
(18) Temtsin, G.; Asefa, T.; Bittner, S.; Ozin, G. A. *J. Mater. Chem.* **2001**, *11*, 3202.
(19) Sayari, A.; Wang, W. *J. Am. Chem. Soc.* **2005**, *127*, 12194.
(20) Muth, O.; Schellbach, C.; Fröba, M. *Chem. Commun.* **2001**, 2032.
(21) Burleigh, M. C.; Markowitz, M. A.; Wong, E. M.; Lin, J.-S.; Gaber, B. P. *Chem. Mater.* **2001**, *13*, 4411.
(22) Bao, X. Y.; Zhao, X. S.; Li, X.; Chia, P. A.; Li, J. *J. Phys. Chem. B* **2004**, *108*, 4684.
(23) Bao, X.; Zhao, X. S.; Li, X.; Li, J. *Appl. Surf. Sci.* **2004**, *237*, 380.
(24) Bao, X. Y.; Zhao, X. S.; Qiao, S. Z.; Bhatia, S. K. *J. Phys. Chem. B* **2004**, *108*, 16441.
(25) Huo, Q.; Margolese, D. I.; Ciesla, U.; Demuth, D. G.; Feng, P.; Gier, T. E.; Sieger, P.; Firouzi, A.; Chmelka, B. F.; Schüth, F.; Stucky, G. D. *Chem. Mater.* **1994**, *6*, 1176.
(26) Huo, Q.; Margolese, D. I.; Stucky, G. D. *Chem. Mater.* **1996**, *8*, 1147.
(27) Guan, S.; Inagaki, S.; Ohsuna, T.; Terasaki, O. *J. Am. Chem. Soc.* **2000**, *122*, 5660.
(28) Guan, S.; Inagaki, S.; Ohsuna, T.; Terasaki, O. *Microporous Mesoporous Mater.* **2001**, *44*−*45*, 165.
(29) Wu, X.; Jin, H.; Liu, Z.; Ohsuna, T.; Terasaki, O.; Sakamoto, K.; Che, S. *Chem. Mater.* **2006**, *18*, 241.
(30) Wang, J.; Xiao, Q.; Zhou, H.; Sun, P.; Yuan, Z.; Li, B.; Ding, D.; Shi, A.; Chen. T. *Adv. Mater.* **2006**, *18*, 3284.
(31) Wang, Y. Q.; Yang, C. M.; Zibrowius, B.; Spliethoff, B.; Lindén, M.; Schüth, F. *Chem. Mater.* **2003**, *15*, 5029.
(32) Liu, X.; Tian, B.; Yu, C.; Gao, F.; Xie, S.; Tu, B.; Che, R.; Peng, L. M.; Zhao, D. Y. *Angew. Chem., Int. Ed.* **2002**, *41*, 3876.
(33) Flodström, K.; Alfredsson, V.; Källrot, N. *J. Am. Chem. Soc.* **2003**, *125*, 4402.
(34) Chan, Y. T.; Lin, H. P.; Mou, C. Y.; Liu, S. T. *Chem. Commun.* **2002**, 2878.
(35) Vartuli, J. C.; Schmitt, K. D.; Kresge, C. T.; Roth, W. J.; Leonowicz, M. E.; McCullen, S. B.; Hellring, S. D.; Beck, J. S.; Schlenker, J. L.; Olson, D. H.; Sheppard, E. W. *Chem. Mater.* **1994**, *6*, 2317.
(36) Tolbert, S. H.; Landry, C. C.; Stucky, G. D.; Chmelka, B. F.; Norby, P.; Handon, J. C.; Monnier, A. *Chem. Mater.* **2001**, *13*, 2247.
(37) Che, S. A.; Kamiya, S.; Terasaki, O.; Tatsumi, T. *J. Am. Chem. Soc.* **2001**, *123*, 12089.
(38) Kim, J.; Ryoo, R. *Chem. Mater.* **1999**, *11*, 487.
(39) Che, S. A.; Lim, S.; Kaneda, M.; Yoshitake, H.; Terasaki, O.; Tatsumi, T. *J. Am. Chem. Soc.* **2002**, *124*, 13962.
(40) Liu, S.; Cool, P.; Callart, O.; Van Der Voort, P.; Vansant, E. F.; Lebedev, O. I.; Van Tendeloo, G.; Jiang, M. *J. Phys. Chem. B* **2003**, *107*, 10405.
(41) Jay, F. L.; Eric, N. J. *J. Org. Chem.* **1994**, *59*, 1939.

(42) Adiam, A.; Moreau, J. J. E.; Wong Chi Man, M. *Chirality* **2000**, *12*, 411.
(43) Foucault, A.; Caude, M.; Oliveros, L. *J. Chromatogr.* **1979**, *185*, 345.
(44) Liu, M.; Sheu, H.; Cheng, S. *Chem. Commun.* **2002**, 2854.
(45) Ogura, M.; Miyoshi, H.; Naik, S. P.; Okubo, T. *J. Am. Chem. Soc.* **2004**, *126*, 10937.
(46) Sakamoto, Y.; Kaneda, M.; Terasaki, O.; Zhao, D.; Kim, J. M.; Stucky, G.; Shin, H. J.; Ryoo, R. *Nature* **2000**, *408*, 449.
(47) Stöber, W.; Fink, A.; Bohn, E. *J. Colloid Interface Sci.* **1968**, *26*, 62.
(48) Ma, Y. R.; Qi, L. M.; Ma, J. M.; Wu, Y. Q.; Liu, O.; Cheng, H. M. *Colloids Surf., A* **2003**, *229*, 1.